

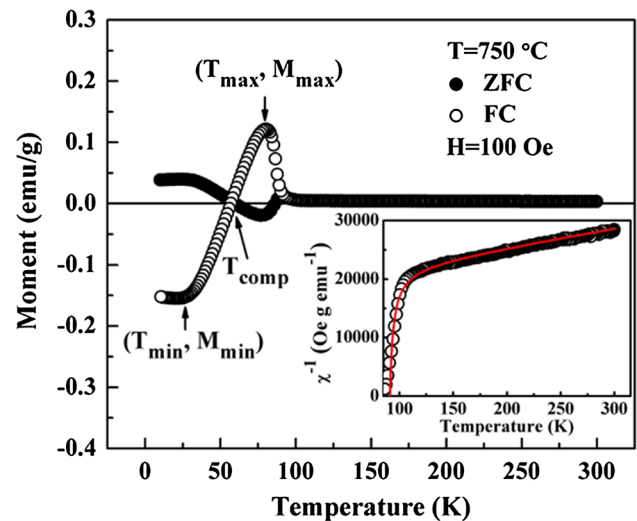
Effect of annealing temperature on negative magnetization behavior in $\text{Co}_{0.775}\text{Cu}_{0.225}\text{Cr}_2\text{O}_4$ ceramics

C. M. Zhu¹ · L. G. Wang¹ · K. Wu¹ · Z. M. Tian¹ · S. L. Yuan¹

Received: 27 February 2016 / Accepted: 1 June 2016 / Published online: 9 June 2016
© Springer Science+Business Media New York 2016

Abstract $\text{Co}_{0.775}\text{Cu}_{0.225}\text{Cr}_2\text{O}_4$ ceramics have been synthesized using the sol–gel method. Through annealed at different temperatures, all the samples are pure formation with cubic crystal structure proved by X-ray diffraction. A significant annealing temperature dependence of negative magnetization has been recorded. With increasing annealing temperature, the absolute values of maximum and minimum of the field-cooled magnetization show a monotonous increase. The relative intensity of negative magnetization is enhanced from 750 to 900 °C and then weakened with further increasing the annealing temperature. The relationship between annealing temperature and negative magnetization can be attributed to the particle growth during the annealing process. In addition, magnetic field dependence of magnetization at 10 K is also studied with different annealing temperatures and the crystallographic microstructure has an important effect on the magnetization.

Graphical Abstract Temperature dependence of magnetization in ZFC and FC processes of $\text{Co}_{0.775}\text{Cu}_{0.225}\text{Cr}_2\text{O}_4$ ceramics annealed at 750 °C. Inset is the FC inverse susceptibility and the fitting of ferrimagnetic Curie–Weiss law down to nearly T_C . Experimental result is plotted as circle, and the fitting is presented as the solid line.



Keywords Sol–gel processes · Annealing temperature · Magnetic properties · Spinels

1 Introduction

Chromium spinel oxides generally written as ACr_2O_4 have a normal cubic structure with the space group of $\text{Fd-}3\text{m}$ at high temperatures. In this structure, A^{2+} cations form a diamond lattice with tetrahedral oxygen environment, while magnetic Cr^{3+} cations surrounded by octahedral oxygen cages form a pyrochlore sublattice [1]. Compared to those members of ACr_2O_4 family, in which Cr^{3+} is the only magnetic cation [2], the presence of magnetic moment in A site may change the magnetic properties in chromium spinel oxides. In accordance with this speculation, we attempt to discuss the magnetic properties of the doped ACr_2O_4 ceramics, in which A^{2+} cations are magnetic.

C. M. Zhu and L. G. Wang have contributed equally to this work.

✉ S. L. Yuan
yuansl@hust.edu.cn

¹ School of Physics, Huazhong University of Science and Technology, Wuhan 430074, People's Republic of China

Magnetization reversal shown as the negative magnetization is usually switched by the direction of applied field, which has been repeatedly observed in many magnetic materials. Different from those systems, one series of materials with orthorhombic structure such as ferrites, vanadates and rare earth chromites can display magnetization reversal induced by temperature [3–5]. Due to fascinating fundamental physics for both information storage and thermomagnetic switches [6], this unusual phenomenon has attracted much attention but it is rarely reported in chromite spinels.

It is widely known that magnetic properties of spinel materials do not only depend on the intrinsic attributes. They can also be sensitive to the preparation technique, which plays a decisive role on crystallization and growth of samples [7]. To begin with, the choice of synthetic methods is a crucial aspect. Sol–gel method operated at low temperature is a cost-effective one. More importantly, it is environmentally friendly relatively. During the synthetic process, a key factor having impact on the magnetic properties is annealing temperature [8]. The variation of annealing temperature can control the formation of the sample microstructures and further affect the magnetic properties of the spinel materials.

Based on the above statements, we report the study about the negative magnetization behavior in $\text{Co}_{0.775}\text{Cu}_{0.225}\text{Cr}_2\text{O}_4$ ceramics. The detailed relationship between negative magnetization and annealing temperature is researched in this paper. $\text{Co}_{0.775}\text{Cu}_{0.225}\text{Cr}_2\text{O}_4$ ceramics can be successfully synthesized with annealing temperature ranging from 750 to 1000 °C. By controlling the annealing temperature, different negative magnetization properties have been realized in $\text{Co}_{0.775}\text{Cu}_{0.225}\text{Cr}_2\text{O}_4$ samples.

2 Experimental procedure

$\text{Co}_{0.775}\text{Cu}_{0.225}\text{Cr}_2\text{O}_4$ ceramics were fabricated by the sol–gel method [9]. Firstly, raw materials of $\text{Co}(\text{NO}_3)_2 \cdot 6\text{H}_2\text{O}$, $\text{Cu}(\text{NO}_3)_2 \cdot 3\text{H}_2\text{O}$, $\text{Cr}(\text{NO}_3)_3 \cdot 9\text{H}_2\text{O}$ and citric acid were dissolved in distilled water with strong magnetic stirring. The solution was maintained at room temperature for 2 h. In this process, citric acid and metal cations have the molar ratio of 1.5:1. Then, pH value of ~ 7 was adjusted by adding ammonia. After that, the solution was thoroughly homogenized to form sol under continuous stirring for about 15 h. Subsequently, the sol was heated in water bath at 100 °C for 5 h to get the gel and then dried in oven at 130 °C for 5 h to form the precursor powders. Finally, the powders were ground in an agate bowl for 2 h and, respectively, annealed at temperatures from 750 to 1000 °C for 3 h to obtain the $\text{Co}_{0.775}\text{Cu}_{0.225}\text{Cr}_2\text{O}_4$ ceramics.

Crystal structures were investigated by X-ray diffraction (XRD, Philips X'pert pro) using the $\text{Cu-K}\alpha$ radiation ($\lambda = 0.15406$ nm) in the 2θ range of 10° – 90° with a step size of 0.02° . Micrographs were measured by scanning electron microscopy (SEM) with a JSM-5610LV. Magnetic measurements were taken through a Physical Property Measurement System (PPMS, Quantum Design).

3 Results and discussion

Figure 1 shows the XRD patterns of $\text{Co}_{0.775}\text{Cu}_{0.225}\text{Cr}_2\text{O}_4$ ceramics. All the samples with different annealing temperatures were pure without any observable impurities. The existence of highest intensity peak around the diffraction angle (2θ) equal to 36° corresponding to (311) plane confirmed the formation of spinel chromite for the samples. Compared with the PDF card numbered 00-022-1084, the ceramics were identified as single phase having a cubic crystal structure with the space group $\text{Fd-}3\text{m}$ at room temperature. All the fundamental peaks were sharp and narrow, which should result from the excellent crystallinity and particle growth by annealing. Calculated by Scherrer's formula, the mean sizes of the crystallites of the samples annealed at 750–1000 °C were, respectively, 73.8, 87, 149.9, 170, 260.8 and 309.1 nm. With increasing the annealing temperature, crystallites presented the monotonous increase. In order to prove this, micrographs of $\text{Co}_{0.775}\text{Cu}_{0.225}\text{Cr}_2\text{O}_4$ ceramics annealed at different temperatures are shown in Fig. 2. It was evident that the particle size increased with increasing annealing temperature. From the micrograph of the sample annealed at 750 °C, we

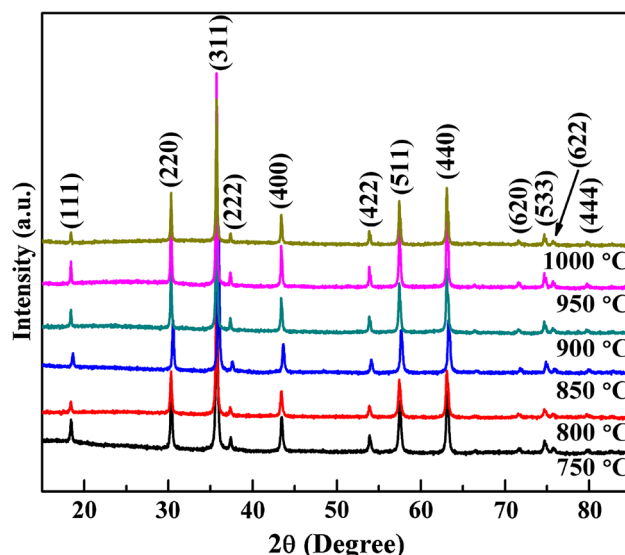


Fig. 1 XRD patterns of $\text{Co}_{0.775}\text{Cu}_{0.225}\text{Cr}_2\text{O}_4$ ceramics annealed at different temperatures

could infer that the particles were nearly spherical shape with fine size at the formation stage. With higher annealing temperature, the mean particle size was bigger with the polyhedral shape. That was consistent with the XRD result obtained as shown in Fig. 1. According to the annealing theory [10], the diffusion among different particles was enhanced with increasing the annealing temperature, which could accelerate the charge and mass transport and further lead to the growth of crystal grains. It could be also proved by the formula of kinetics about the grain growth

$$d_g^n = Ct \exp\left(-\frac{E}{RT}\right), \quad (1)$$

where d_g was the average grain size, n was the dynamic index of grain growth, t was the annealing time, E was the activation energy of grain growth and T was the annealing temperature. In addition, C and R were constants [11]. According to the expression of formula, we could also confirm that the particle size was increasing with increasing annealing temperature. On the other hand, the bigger particle size and the crystallographic polyhedral formation

with increasing annealing temperature did not generate the homogeneous microstructure of the samples; especially, annealed at higher temperatures, the micrographs showed an evident agglomeration phenomenon. So, it was really intriguing to find out the influence of annealing temperature on the magnetic properties of $\text{Co}_{0.775}\text{Cu}_{0.225}\text{Cr}_2\text{O}_4$ ceramics.

As shown in Fig. 3, temperature dependence of magnetization in zero-field-cooled (ZFC) and field-cooled (FC) processes was measured with $H = 100$ Oe for $\text{Co}_{0.775}\text{Cu}_{0.225}\text{Cr}_2\text{O}_4$ ceramics. All the samples followed the typical ferrimagnetic transition (T_C) at ~ 91 K [12]. Insets of Fig. 3 are FC inverse susceptibility and the fitting of ferrimagnetic Curie–Weiss law down to nearly T_C of the different samples [13, 14]. The experimental susceptibility (χ) was obtained by M/H , where M was magnetization and H was the applied field [15]. The inverse susceptibility (χ^{-1}) was also obtained as the reciprocal of magnetic susceptibility. χ^{-1} followed the hyperbolic behavior characteristic of ferrimagnets described as below:

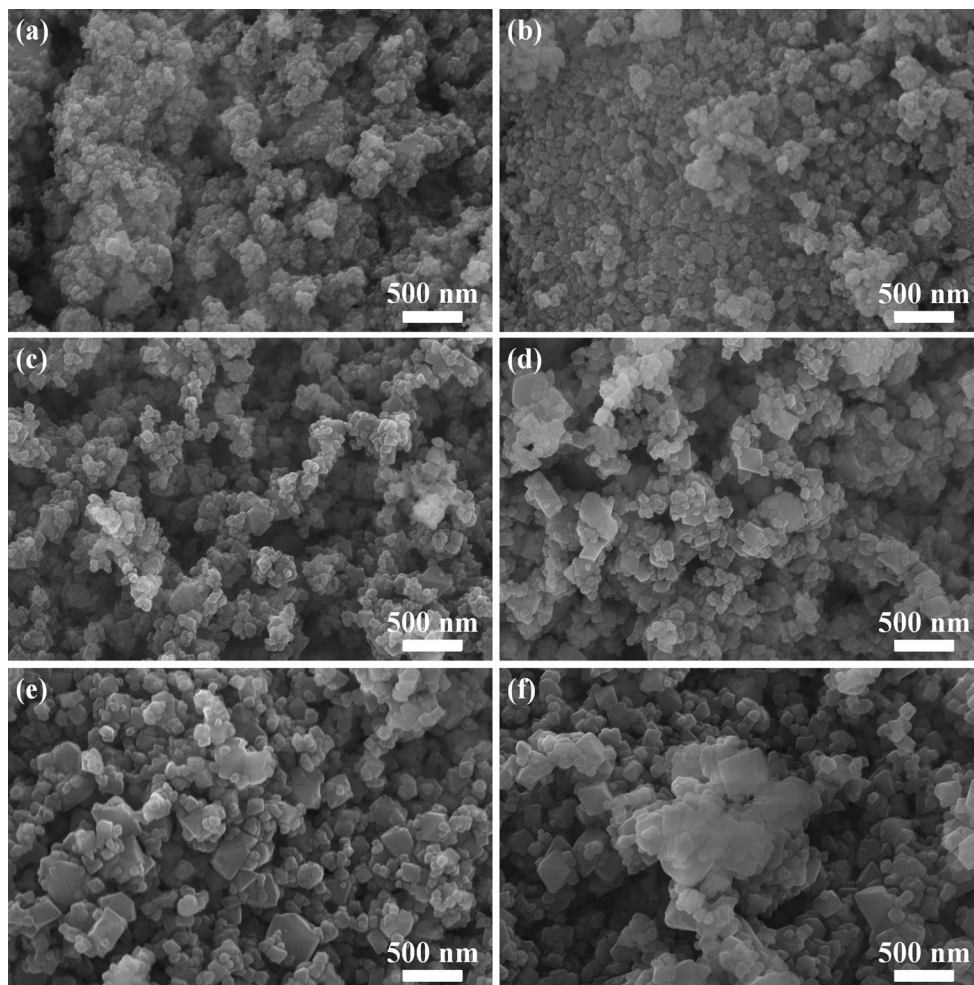


Fig. 2 SEM micrographs of $\text{Co}_{0.775}\text{Cu}_{0.225}\text{Cr}_2\text{O}_4$ ceramics annealed at **a** 750, **b** 800, **c** 850, **d** 900, **e** 950 and **f** 1000 °C

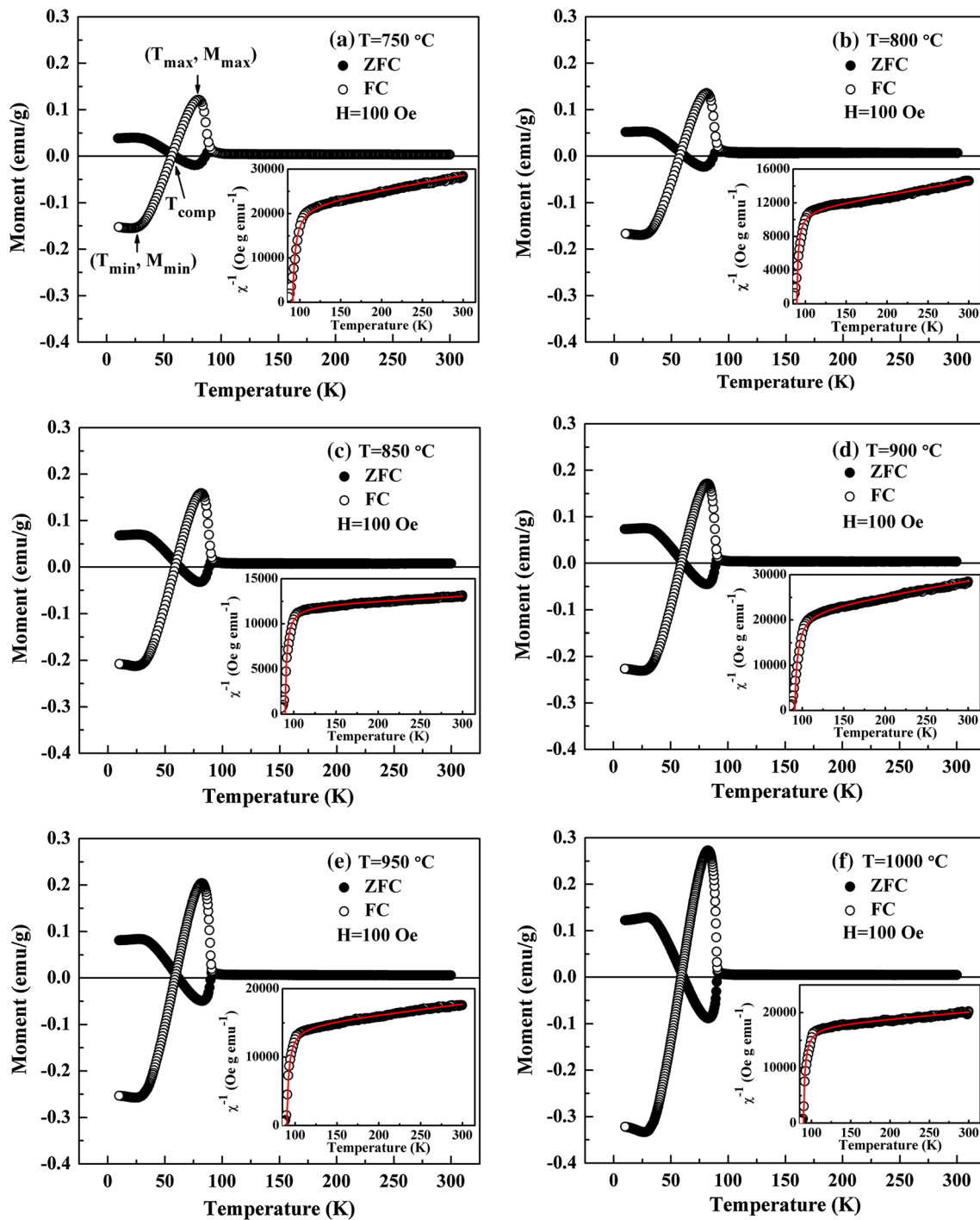


Fig. 3 Temperature dependence of magnetization in ZFC and FC processes of $\text{Co}_{0.775}\text{Cu}_{0.225}\text{Cr}_2\text{O}_4$ ceramics annealed at **a** 750, **b** 800, **c** 850, **d** 900, **e** 950 and **f** 1000 °C. *Insets* are the FC inverse

susceptibility and the fitting of ferrimagnetic Curie–Weiss law down to nearly T_C . Experimental result is plotted as circle, and the fitting is presented as the *solid line*

$$\chi^{-1}(T) = [(T - \Theta)/C] - [\xi/(T - \Theta)'], \quad (2)$$

where the first term was the hyperbole asymptote at the high-temperature range which had a Curie–Weiss form [16]. Extrapolated from the fitting line, T_C could be defined

as the temperature at which the χ^{-1} was zero. The values of fitting T_C were, respectively, 91.3, 89.8, 90.2, 90.6, 90.5 and 90.3 K with annealing temperature at 750–1000 °C. All of the fitting values of T_C were about 91 K. It further confirmed the experimental transition temperature at

~91 K as shown in Fig. 3. With the decrease in measuring temperature, magnetization of ZFC and FC curves presented the clear irreversibility, indicating the strong magnetocrystalline anisotropy in the samples. It should be related to the random distribution of net moments in polycrystalline $\text{Co}_{0.775}\text{Cu}_{0.225}\text{Cr}_2\text{O}_4$ ceramics and the non-collinear moments with doping of Cu. Further lowering measuring temperature from ferrimagnetic transition point, magnetization of FC curves had a sharp rise, obtained the maximum and then dropped down passing through the zero value of magnetization at a special temperature. The temperature point was named as the compensation temperature (T_{comp}) as shown in Fig. 3(a). It was the sign of magnetization reversal, at which the magnetic poles could invert [17]. Generally, the appearance of T_{comp} in FC curves was accompanied with the negative magnetization, displaying as the positive magnetization above T_{comp} , zero value of magnetization at T_{comp} and negative value of magnetization below T_{comp} . In our samples, FC magnetization took on the negative value and displayed the minimum at a lower-temperature range below T_{comp} . Here, to be convenient for explanation and comparison, we defined the maximum of positive value in FC magnetization curves as M_{max} . Accordingly, the temperature, at which M_{max} was obtained, was defined as the T_{max} . Similarly, the M_{min} was on behalf of the minimum of FC magnetization with negative value. The temperature with M_{min} is named as T_{min} . The details are shown in Fig. 3a. In our samples, negative value of FC magnetization revealed that the moment direction was antiparallel to the direction of applied field. It meant that negative magnetization behavior could be generated in $\text{Co}_{0.775}\text{Cu}_{0.225}\text{Cr}_2\text{O}_4$ ceramics annealed at temperatures ranging from 750 to 1000 °C. What was more, this magnetization reversal between positive and negative values was realized only by measuring temperature. This phenomenon did not appear in CoCr_2O_4 samples of so many

previous researches. It should be noted that negative value was also found in ZFC magnetization, which could be attributed to the uncompensated spins at the grain boundaries of polycrystalline samples [18]. As known in the system of ferrimagnetic spinels, magnetization was strongly influenced by the site preference of the cations in structure lattices. It was usually explained on the basis of magnetic interaction among the metal cations located in the two crystallographic sites including tetrahedral A sublattice and octahedral B sublattice, respectively [19, 20]. In consideration of the crystallographic and magnetic structure of the samples, we explained the negative magnetization behavior according to the different temperature dependence of the sublattice magnetization based on the two-sublattice model. Co^{2+} and Cu^{2+} cations were preferentially occupying A sublattices with ferromagnetic interaction bringing about the positive moments, while Cr^{3+} cations had a strong preference to occupying B sublattices with antiferromagnetic interaction giving rise to the antiparallel moments to the direction of applied field. The different temperature dependence of sublattice magnetization emerged as that the magnetization maximum in FC curves was only from A sublattices. Antiparallel moments of B sublattices contributing to negative magnetization just started from the decrease in FC magnetization. This arrangement resulted in the competition between A and B sublattice magnetization leading to the negative magnetization behavior in $\text{Co}_{0.775}\text{Cu}_{0.225}\text{Cr}_2\text{O}_4$ ceramics. Besides these intrinsic factors, magnetization could be also affected by some extrinsic factors such as the annealing temperature. Moreover, there was no relevant research mentioning the relationship between negative magnetization and annealing temperature. As shown in Fig. 3, FC magnetization value was indeed influenced by the annealing temperature; especially, both the M_{max} obtained from

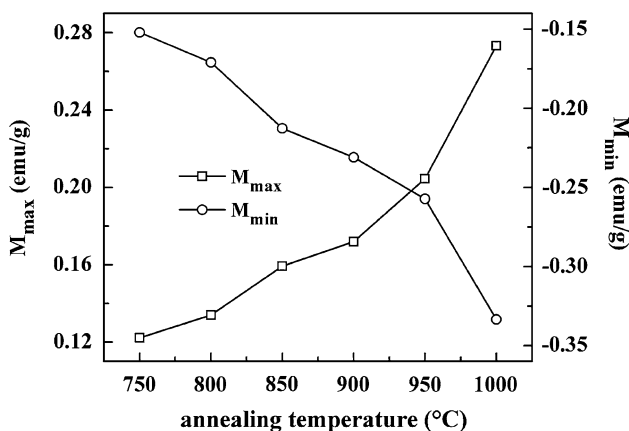


Fig. 4 Evolutions of M_{max} and M_{min} with the increasing annealing temperature

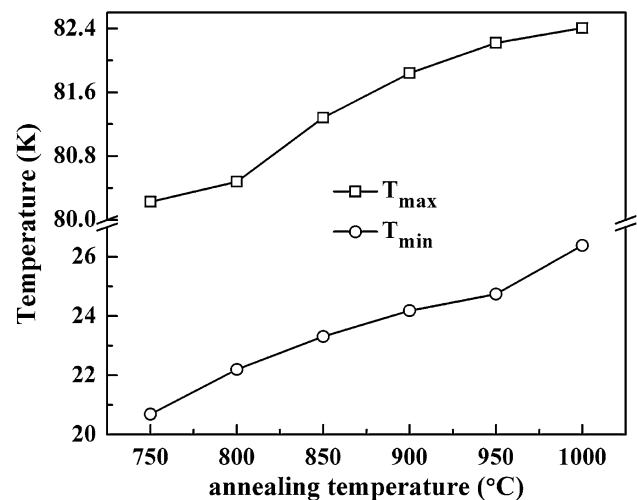


Fig. 5 Evolutions of T_{max} and T_{min} with the increasing annealing temperature

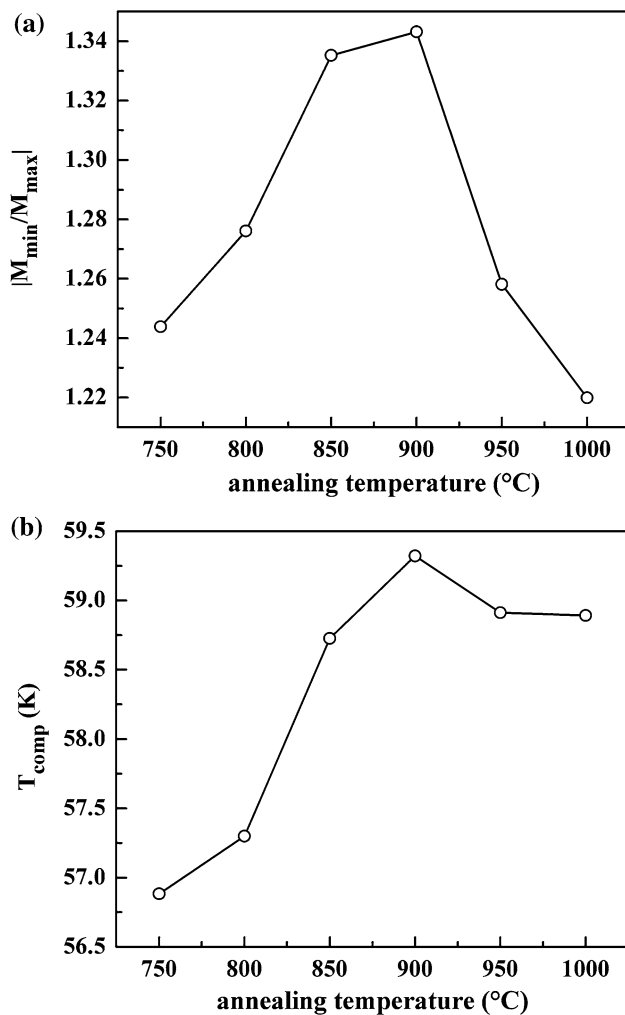


Fig. 6 Evolutions of $|M_{\min}/M_{\max}|$ (a) and T_{comp} (b) with the increasing annealing temperature

ferromagnetic interaction of A sublattices and the M_{\min} mainly governed by the antiparallel moments of B sublattices had a monotonous change tendency with increasing annealing temperature. In order to clearly see the variation characteristics of negative magnetization, we plotted the different parameter change with the increasing annealing temperature. Figure 4 shows the variation of M_{\max} and M_{\min} with increasing annealing temperature. M_{\max} increased from ~ 0.122 emu/g annealed at 750 °C to ~ 0.273 emu/g at 1000 °C. M_{\min} decreased from about -0.152 emu/g at 750 °C to about -0.333 emu/g at 1000 °C, which could be regarded as that the absolute value of M_{\min} ($|M_{\min}|$) was also increased with increasing annealing temperature. XRD results manifested that annealing temperature did not change the crystal structure of $\text{Co}_{0.775}\text{Cu}_{0.225}\text{Cr}_2\text{O}_4$ ceramics. So, the magnetization change with increasing annealing temperature should be ascribed to the change in microstructure and morphology of the samples. As shown in Fig. 2, a distinct change of the

samples was the monotonously increasing particle size as annealing temperature increases. The consistent and monotonous change tendency between particle size and FC magnetization made the speculation possible that the increase in M_{\max} and $|M_{\min}|$ was mainly related to the growth of particle size. Samples annealed at low temperature had the small particle size with relatively poor crystallinity, which could diminish the surface strain resulting in the lattice disorder at the particle surface. The disorder would produce the increased fraction of surface atoms and the reduced crystal symmetry due to the incomplete atomic coordination. Hence, small particles with large ratio of surface to volume possessed the incomplete spin periodicity with net moments due to the poor crystallinity. That was, the major contribution to magnetization annealed at low temperature was just from the uncompensated spins at the small particle surface. On the other hand, the disorder in small particles with poor crystallinity could hinder the formation and growth of magnetic domains, which also led to the low magnetization annealed at low temperature. With increasing annealing temperature, the particle size was gradually increased and the crystallinity was also enhanced [21, 22]. Accordingly, the surface area was steadily decreased accompanied with the growth of magnetic domains. As shown in Fig. 2, agglomerate phenomenon always existed in the samples with increasing annealing temperature. The agglomerate particles through annealing process might be also presented with some defects such as the pores influenced by oxygen content. However, the monotonous increase in M_{\max} and $|M_{\min}|$ indicated that the agglomeration with possible defects had negligible effect on the measured magnetization in FC process. Moreover, all the samples were annealed in air atmosphere adequately at different temperatures with enough annealing time. So, Co and Cu cations in the samples should be mainly Co^{2+} and Cu^{2+} , and the valence influence of Co and Cu cations on magnetization could be also negligible. The monotonous variation of M_{\max} and $|M_{\min}|$ with increasing annealing temperature could also prove the discussion. In addition, T_{\max} and T_{\min} also showed the increasing trend as annealing temperature increases. In Fig. 5, T_{\max} increased from ~ 80.225 K at 750 °C to ~ 82.407 K at 1000 °C and T_{\min} increased from ~ 20.695 K at 750 °C to ~ 26.375 K at 1000 °C. The increasing particle size gave an important improvement in FC magnetization of the samples. It revealed that the samples did not need to get a stronger magnetization at a relative lower measuring temperature with the increase in annealing temperature, thus exhibiting the corresponding increase in T_{\max} and T_{\min} . However, $|M_{\min}/M_{\max}|$ was initially increased from 750 to 900 °C and then decreased from 900 to 1000 °C as shown in Fig. 6a. Here, $|M_{\min}/M_{\max}|$ was the absolute value of M_{\min}/M_{\max} .

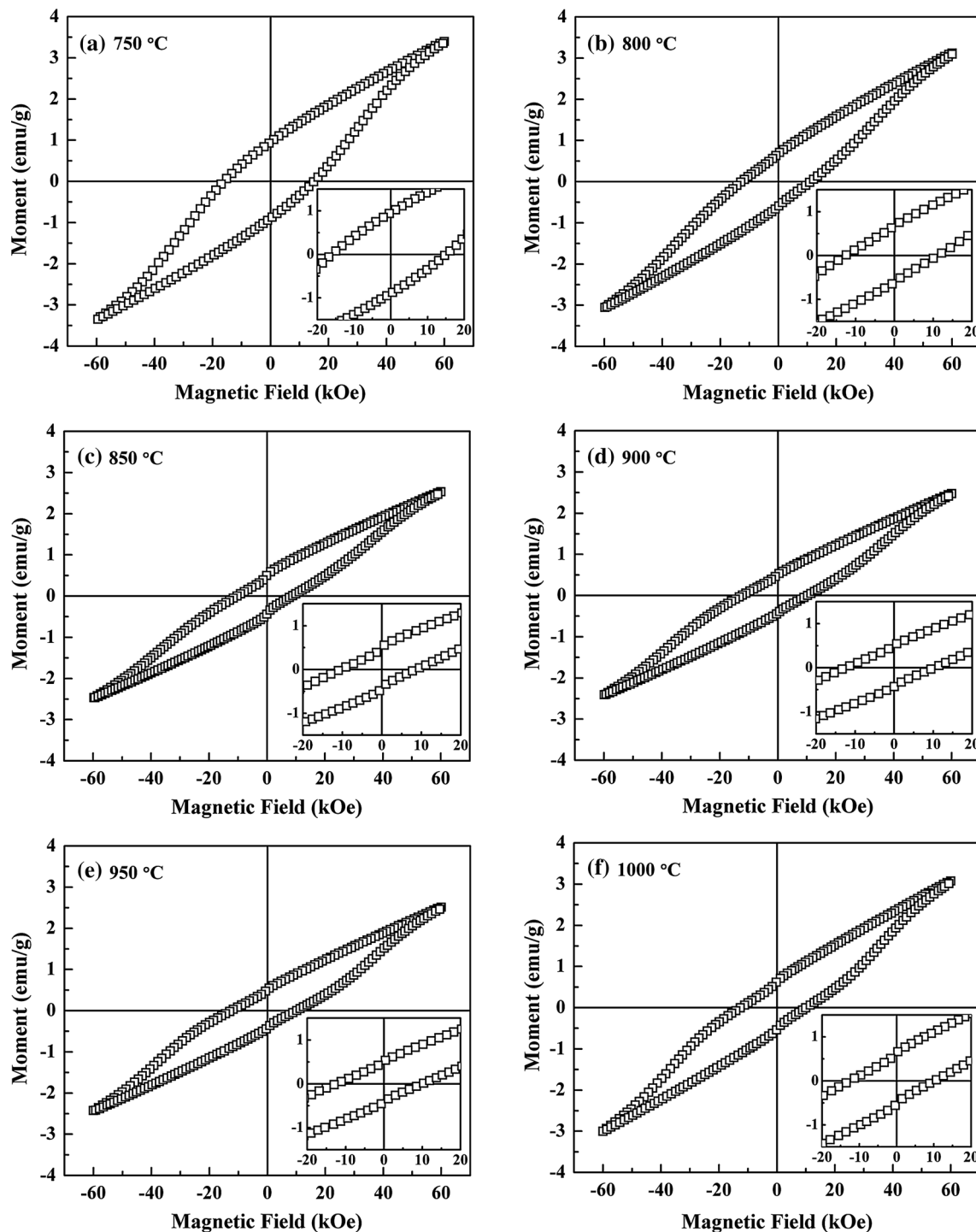


Fig. 7 Magnetic hysteresis loops at 10 K for $\text{Co}_{0.775}\text{Cu}_{0.225}\text{Cr}_2\text{O}_4$ ceramics annealed at **a** 750, **b** 800, **c** 850, **d** 900, **e** 950 and **f** 1000 °C. *Insets* are the magnified patterns of magnetic hysteresis loops of different samples

Because the total magnetization of the samples was changed with the annealing temperature including the positive value and negative value, the M_{\min} shown in FC curves was just the observable value of negative magnetization. It was not sufficient to present the relative intensity of negative magnetization behavior of the samples. So, referring to the

previous study [23], we defined the $|M_{\min}/M_{\max}|$ as the representative of negative magnetization behavior. As the relative intensity of negative magnetization, $|M_{\min}/M_{\max}|$ could display the change of negative magnetization behavior more clearly. As annealing temperature increases, $|M_{\min}/M_{\max}|$ was not enhanced monotonously with the

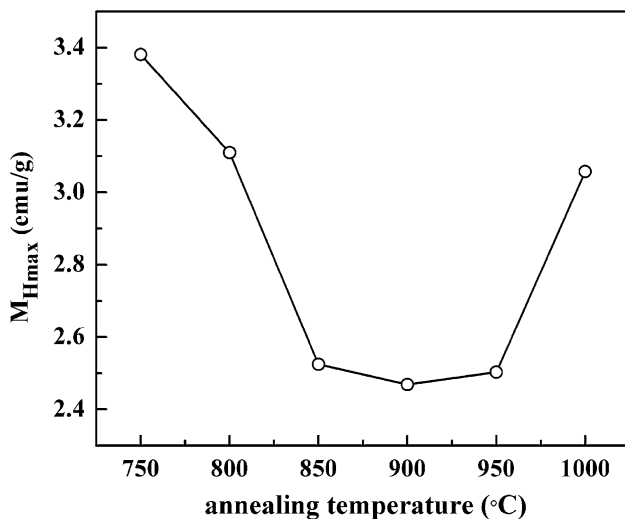


Fig. 8 Evolutions of $M_{H_{\max}}$ with the increasing annealing temperature increase in annealing temperature. The increasing particle size enhanced the FC magnetization containing both positive and negative value, but the two kinds of values coming from two sublattices did not have the similar increasing rate with increasing annealing temperature. As a result, the maximum of $|M_{\min}/M_{\max}|$ was from the sample annealed at 900 °C. As the other important parameter of negative magnetization behavior, T_{comp} demonstrated the similar change tendency to $|M_{\min}/M_{\max}|$ as shown in Fig. 6b, which was the variation of T_{comp} with annealing temperature. T_{comp} increased from ~ 56.884 K at 750 °C to ~ 59.322 K at 900 °C and then dropped to ~ 58.893 K at 1000 °C. The highest T_{comp} was also at 900 °C. The change tendency of $|M_{\min}/M_{\max}|$ indicated that the negative moments of B sublattices increased faster than the positive moments of A sublattices with annealing temperature increasing from 750 to 900 °C. It was meaning that negative value could offset the positive value at a higher temperature with increasing annealing temperature. Once exceeding 900 °C, magnetization of B sublattices changed gradually slowly compared with the A sublattice magnetization; thus, $|M_{\min}/M_{\max}|$ decreased and the offset point of the magnetization accordingly shifted toward to a lower temperature from 900 to 1000 °C. That was to say, the change tendency of T_{comp} with increasing annealing temperature was also attributed to the magnetization variation in A and B sublattices as annealing temperature rose.

Figure 7 shows the magnetic hysteresis loops at 10 K for the samples annealed at different temperatures. Magnetic properties were successfully realized with the well-defined hysteresis loops. The detailed magnetic hysteresis loops at low field value are, respectively, shown in the insets of the different samples in Fig. 7. It could be found that all the hysteresis loops were symmetric around the origin [24, 25]. It was worth noting that the loops were not

saturated in the field of 60 kOe. The antiferromagnetic interaction between Cr^{3+} cations could contribute to this phenomenon. Regardless of the annealing temperature, all the hysteresis loops revealed the almost similar remnant magnetization and coercive field. Unlike these two parameters, the maximum field magnetization ($M_{H_{\max}}$) defined as the magnetization in the field of 60 kOe was affected by the annealing temperature. Evident annealing temperature dependence of $M_{H_{\max}}$ was vivid as shown in Fig. 8. Obviously, $M_{H_{\max}}$ showed an initial decrease from ~ 3.381 emu/g at 750 °C to ~ 2.469 emu/g at 900 °C and then increased to ~ 3.058 emu/g at 1000 °C. We had stated that the change of negative magnetization behavior in FC curves was mainly due to the increasing particle size. However, when annealing temperature increased from 750 to 900 °C, $M_{H_{\max}}$ at 10 K dropped sharply with an inflexion at 900 °C. This should be not the only result of the increasing particle size. Besides particle size, increasing annealing temperature also led to the different crystallinity and growth of the samples. The homogeneous arrangement of crystal structure in magnetic materials had the essential responsibility for the magnetic order which made the materials magnetic. As shown in Fig. 2, particle size increased with increasing annealing temperature, but the microstructure was anomalous. Microstructure with agglomerates began to find with annealing temperature increasing from 800 °C. The appearance of agglomerates represented that there were defects such as pores in the ceramic samples. Those pores acted as pinning centers for the electron spins to impede the moment rotation, thereby lowering the magnetization. As annealing temperature further increased from 900 °C, annealing effect led to the particle growth and pore elimination due to densification. The larger particles made the formation of domain walls possible with a greater number of the domain walls in the samples. The magnetization caused by domain wall movement required less energy than that required by domain rotation [26]. As the number of walls increased with particle size, the contribution of wall movement to magnetization was greater than that of domain rotation. Due to the domain wall movement under the action of the magnetic field, magnetization would increase. That was, they could be attributed to the increase in average particle size and the bulk density.

4 Conclusions

In conclusion, we have mainly studied the annealing temperature dependence of negative magnetization behavior in $\text{Co}_{0.775}\text{Cu}_{0.225}\text{Cr}_2\text{O}_4$ ceramics. Negative magnetization appears in $\text{Co}_{0.775}\text{Cu}_{0.225}\text{Cr}_2\text{O}_4$ ceramics annealed at

temperatures from 750 to 1000 °C. Magnetization in FC curves displays the evident dependent phenomenon on the annealing temperature. M_{\max} and $|M_{\min}|$ in FC curves increase monotonously with increasing annealing temperature accompanied by the increasing T_{\max} and T_{\min} . Through analyzing the relative intensity of negative magnetization and the compensation temperature, the two parameters of negative magnetization behavior obtain the maximums at 900 °C. We have also measured the magnetic hysteresis loops at 10 K with different annealing temperatures. Magnetic properties are well realized, and $M_{H_{\max}}$ also shows the evident dependence on the annealing temperature. We attribute the relationship between annealing temperature and negative magnetization behavior to the microstructure variation including the particle growth and the crystallization of the samples. Our results help in understanding the controversies in the negative magnetization of $\text{Co}_{0.775}\text{Cu}_{0.225}\text{Cr}_2\text{O}_4$ ceramics. Of course, more studies should be carried out to give the detailed information of the underlying mechanisms.

Acknowledgments This work was supported by the National Natural Science Foundation of China (Grant No. 11474111). We would like to thank the staff of Analysis Center of HUST for their assistance in various measurements.

References

- Ptak M, Maczka M, Gagor A, Pikul A, Macalik L, Hanuza J (2013) Temperature-dependent XRD, IR, magnetic, SEM and TEM studies of Jahn–Teller distorted NiCr_2O_4 powders. *J Solid State Chem* 201:270–279
- Kagomiya I, Toki M, Kohn K, Hata Y, Kita E, Siratori K (2004) Magnetic clusters in three dimensional spin frustrated system ZnCr_2O_4 . *J Magn Magn Mater* 272–276:e1031–e1032
- Yuan SJ, Ren W, Hong F, Wang YB, Zhang JC, Bellaiche L, Cao SX, Cao G (2013) Spin switching and magnetization reversal in single-crystal NdFeO_3 . *Phys Rev B* 87:184405
- Ren Y, Palstra TTM, Khomskii DI, Pellegrin E, Nugroho AA, Menovsky AA, Sawatzky GA (1998) Temperature-induced magnetization reversal in a YVO_3 single crystal. *Nature* 396:441–444
- Yoshii K (2012) Magnetization reversal in TmCrO_3 . *Mater Res Bull* 47:3243–3248
- Cao YM, Cao SX, Ren W, Feng ZJ, Yuan SJ, Kang BJ, Lu B, Zhang JC (2014) Magnetization switching of rare earth orthochromite CeCrO_3 . *Appl Phys Lett* 104:232405
- Ismail I, Hashim M, Ibrahim IR, Nazlan R, Idris FM, Shafie SE, Manap M, Bahmanrokh G, Abdullah NH, Rahman WNW (2013) Crystallinity and magnetic properties dependence on sintering temperature and soaking time of mechanically alloyed nanometer-grain $\text{Ni}_{0.5}\text{Zn}_{0.5}\text{FeO}_4$. *J Magn Magn Mater* 333:100–107
- Zhu CM, Wang LG, Tian ZM, Luo H, Bao DLGC, Yin CY, Huang S, Yuan SL (2016) Effect of annealing temperature on the multiferroic properties of $0.7\text{BiFeO}_3\text{-}0.3\text{Bi}_{0.5}\text{Na}_{0.5}\text{TiO}_3$ solid solution prepared by sol–gel method. *Ceram Int* 42:3930–3937
- Wang LG, Zhu CM, Luo H, Yuan SL (2015) Studies on room temperature multiferroic properties of $x\text{Bi}_{0.5}\text{Na}_{0.5}\text{TiO}_3\text{-}(1-x)\text{NiFe}_2\text{O}_4$ ceramics. *J Electroceram* 35:59–67
- Radecka M, Rekas M (2002) Charge and mass transport in ceramic TiO_2 . *J Eur Ceram Soc* 22:2001–2012
- Senda T, Bradf RC (1990) Grain growth in sintered ZnO and $\text{ZnO-Bi}_2\text{Fe}_3$ ceramics. *J Am Ceram Soc* 73:106–114
- Bordács S, Varjas D, Kézsmárki I, Mihály G, Baldassarre L, Abouelsayed A, Kuntscher CA, Ohgushi K, Tokura Y (2009) Magnetic-order-induced crystal symmetry lowering in ACr_2O_4 ferrimagnetic spinels. *Phys Rev Lett* 103:077205
- Tadic M, Milosevic I, Kralj S, Mbodji M, Motte L (2015) Silica-coated and bare akaganeite nanorods: structural and magnetic properties. *J Phys Chem C* 119:13868–13875
- Tadic M, Nikolic D, Panjan M, Blake GR (2015) Magnetic properties of NiO (nickel oxide) nanoparticles: blocking temperature and Neel temperature. *J Alloy Compd* 647:1061–1068
- Yoshii K, Nakamura A (2000) Reversal of magnetization in $\text{La}_{0.5}\text{Pr}_{0.5}\text{CrO}_3$. *J Solid State Chem* 155:447–450
- Winkler E, Canosa SB, Rivadulla F, López-Quintela MA, Rivas J, Caneiro A, Causa MT, Tovar M (2009) Magnetocrystalline interaction in MnCr_2O_4 spinel. *Phys Rev B* 80:104418
- Ohkoshi S, Abe Y, Fujishima A, Hashimoto K (1999) Design and preparation of a novel magnet exhibiting two compensation temperatures based on molecular field theory. *Phys Rev Lett* 82:1285–1288
- Kumar N, Sundaresan A (2010) On the observation of negative magnetization under zero-field-cooled process. *Solid State Commun* 150:1162–1164
- Staruch M, Hires D, Violette D, Navarathne D, Sotzing GA, Jain M (2011) Structural and magnetic properties of CoFe_2O_4 and $\text{Co}_{0.5}\text{Zn}_{0.5}\text{Fe}_2\text{O}_4$ nanoparticles for the magnetoelectric composite films, *Integr. Ferroelectrics* 131:102–109
- Choi YJ, Okamoto J, Huang DJ, Chao KS, Lin HJ, Chen CT, van Veenendaal M, Kaplan TA, Cheong S-W (2009) *Phys Rev Lett* 102:067601
- Lee J, Park JY, Kim CS (1998) Growth of ultra-fine cobalt ferrite particles by a sol–gel method and their magnetic properties. *J Mater Sci* 33:3965–3968
- Eum YJ, Hwang SO, Koo CY, Lee JY, Lee HY, Ryu J, Park JM (2014) Effect of annealing temperature on the magnetoelectric properties of $\text{CoFe}_2\text{O}_4/\text{Pt/Pb}(\text{Zr}_{0.52}\text{Ti}_{0.48})\text{O}_3$ multilayer films. *J. Korean Phys Soc* 65:342–345
- Lakhani VK, Zhao BC, Wang L, Trivedi UN, Modi KB (2011) Negative magnetization, magnetic anisotropy and magnetic ordering studies on Al^{3+} -substituted copper ferrite. *J Alloy Compd* 509:4861–4867
- Tadic M, Kusigerski V, Markovic D, Milosevic I, Spasojevic V (2009) High concentration of hematite nanoparticles in a silica matrix: structural and magnetic properties. *J Magn Magn Mater* 321:12–16
- Tadić M, Spasojević V, Kusigerski V, Marković D, Remškar M (2008) Formation of $\epsilon\text{-Fe}_2\text{O}_3$ phase by the heat treatment of $\alpha\text{-Fe}_2\text{O}_3/\text{SiO}_2$ nanocomposite. *Scr Mater* 58:703–706
- Zabotto FL, Gualdi AJ, Eiras JA, Oliveira AJA, Garcia D (2012) Influence of the sintering temperature on the magnetic and electric properties of NiFe_2O_4 ferrites. *Mater Res* 15:428–433